

## A Model for Saharan Dust Transport

GUILLAUME A. D'ALMEIDA\*

*Meteorologisches Institut der Universität München, 8000 Munich 2, F.R.G.*

(Manuscript received 1 August 1985, in final form 12 December 1985)

### ABSTRACT

In this paper the source strength and the deposition rate of the dust emerging from the Sahara are assessed. For this purpose a multichannel sunphotometer has been developed and a turbidity network covering 11 stations has been set up in the Sahara, in the Sahel region and the surrounding southern area for a duration of about two years. A correlation analysis connecting observed aerosol turbidity parameters and mineral dust mass concentration has been performed during a four-week field campaign in Agadez (Niger). An appropriate box model including the aerosol turbidity parameters, actual wind field data of the source regions, the general circulation pattern over Africa and dry and wet deposition reveals a total mass production of about  $630 \times 10^6$  and  $710 \times 10^6 \text{ t yr}^{-1}$  for all suspended particulate matter,  $80 \times 10^6$  and  $90 \times 10^6 \text{ t yr}^{-1}$  for aerosol particles smaller than  $5 \mu\text{m}$  radius for the years 1981 and 1982 respectively. About 60% of the mass moves southward to the Gulf of Guinea, 28% westward to the equatorial North Atlantic Ocean and 12% northward to Europe. A considerable part is deposited in the Atlantic Ocean and the Mediterranean forming deep-sea sediments.

### 1. Introduction

To compute the radiative field on a global scale, space and time distributions of the extinction coefficient, the single scattering albedo, the anisotropy factor or phase function and the optical depth of the aerosol type considered are necessary. The direct and indirect influence of aerosol particles on climate, mostly expressed in terms of energy balance, can be estimated, when mass concentration or source strength of the different aerosol types is known.

Most of the aerosol or climate models, in which aerosol particles are incorporated, ignore or consider the mineral component of the tropospheric aerosols with needy parameters (e.g., DeLuisi et al., 1972; Toon and Pollack, 1976; Hänel and Bullrich, 1978; Shettle and Fenn, 1979; WCP-55, 1983; Lenoble and Brogniez, 1984; Tanre et al., 1984) although arid and semiarid regions of the world cover about 36% of the Earth's land surface (Meigs, 1953). This shortcoming is probably due to the lack of information. In a previous introductory paper (d'Almeida and Schütz, 1983), the size distribution of mineral aerosols during different weather conditions was presented. With a suitable choice of the wavelength-dependent, particle refractive-index the aforementioned, climate relevant, radiative parameters can be computed. This has been done and will be published elsewhere. Encouraged by the results, we have decided to continue our investigation by de-

termining the source strength of particulate matter emerging from the Sahara.

Another reason supporting our aim is of environmental or ecological concern. The Sahelian drought in the 1970s and following years and the subsequent famine lead to the belief of an obvious climate change due either to manmade activities, or natural causes or both. A long-term study of the seasonal shift of the climatic belts, especially the Intertropical Convergence Zone (ITCZ), the desert surface temperature and, of course, the dust activity may reveal a reliable trend.

Knowledge about source strength and deposition rate of different aerosol types, especially of mineral dust, is limited. Peterson and Junge (1971) estimated the global contribution of wind-blown dust derived from soil erosion to be approximately  $500 \times 10^6 \text{ t yr}^{-1}$ . Their rough calculation was based on average concentrations and residence time. For the purpose of estimating the average global albedo and the Earth's surface temperature, Joseph et al. (1973) computed the dust mass transported during a weather phenomenon called "Kham-sin." In that report the method and feasibility of such a study are more important to stress than the finding. The latter is namely related to a single dust episode. Rather, the estimation of the Saharan dust component transported over the North Atlantic Ocean, termed westward transport, conducted by Prospero and Carlson (1972), Schütz (1977), Jaenicke and Schütz (1978) is based on reliable computations and a long-term investigation. Some differences, however, have been noted in their model results. As for the transport of Saharan dust toward the Gulf of Guinea (South trans-

\* Former affiliation: Johannes Gutenberg Universität, Institut für Meteorologie, 6500 Mainz, F.R.G.

port) and Europe (North transport), no study is available so far. The presentation of a model yielding the total production and deposition rate of the dust emerging from the Sahara is the purpose of this paper.

## 2. Source areas of Saharan dust

In this report we call source areas of mineral dust those regions in the desert from which most of the airborne particulate matter originates. Their location is the subject of controversial discussions in the open literature. Indeed, the geomorphology of arid regions is rather complex, comprising rock deserts, gravelly soils, loamy soils, salt deserts, sandy deserts and a mixture of the different types. Their dust productivity is largely variable (d'Almeida and Schütz, 1983). For a tentative identification of important source areas, satellite observations, comparison of element composition, comparison of aerosol and soil sample color, monitoring of air mass trajectory and visibility distribution analyses are useful methods. Among them, visibility analysis for unaged aerosol particles seems to be the easiest and most common technique, to date. Many authors (Bertrand et al., 1974; d'Almeida, 1979; Kalu, 1979; Morales, 1979, 1981) use this facility to follow the generation and migration of dust plumes. However, due to severe climatic and vital conditions, ground truth observations in the Sahara are rather sporadic. Visibility estimations on synoptic weather maps are, therefore, only reported for selected stations located one to two days travel distance from the real source areas. It is obvious that, with respect to source area location, a visibility distribution based on aged aerosol particles

may yield an artifact. For instance, we were told by observers that Bilma (Niger) had never been a source region as Kalu (1979) reported.

The following consideration of source areas is also based on several trips and comprehensive discussions with resident observers of stations in the Sahara and Sahel regions and supported by the United Nation's map for soil erosion in Africa entitled "Provisional Methodology for Soil Degradation Assessment," published by FAO, UNEP and UNESCO.

Four major source areas, as roughly shown in Fig. 1, are stated in this model. Source 1 extends from the Spanish Sahara to North Mauritania. Source 2 is located in the triangle formed by the Hoggar, Adrar des Iforhas and Air mountains, i.e., northeast of Gao (Mali). Source 3 is situated north to northeast of Dirku, north of Bilma (Niger) off the west side of the Tibesti Mountains in Chad. Source 4 is located in the northern part of Sudan. According to the United Nation's map, these areas seem to be the most productive in the Sahara. It is not intended to give rise to the belief that the identified source areas are unique or mandatory. Of course, many secondary areas also exist such as the sand mass in the vicinity of In Salah (Algeria), Djebock (Mali), Mersa Matruh (Egypt), or the alluvial land in the regions of Goundam (Mali), Matan (Senegal) and elsewhere. Their productivity, however, appears to be relatively negligible. Most of them are obviously depleted or attenuated, or the smoothness condition does not permit effective wind erosion to take place. The exact geographic location and areas of the major sources are deduced from the aforementioned United Nation's map for soil erosion.

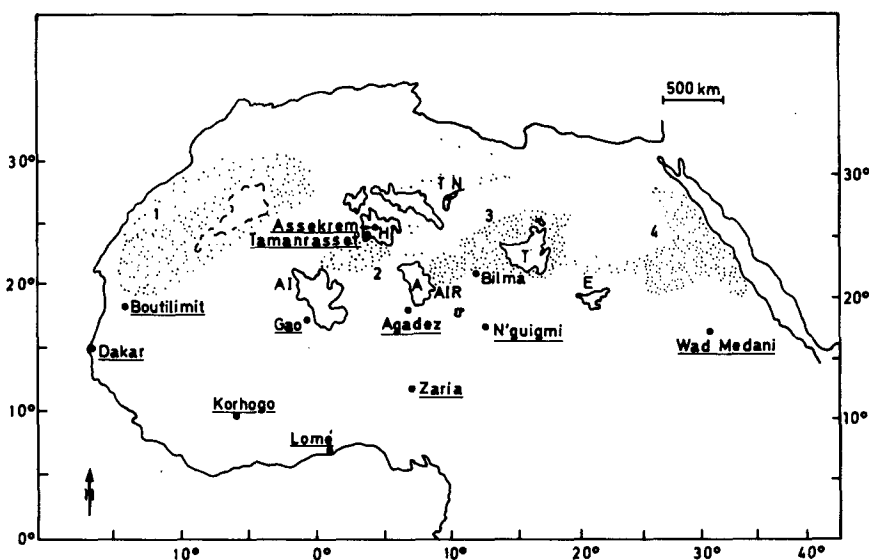


FIG. 1. Location of the major source areas for airborne Saharan dust and presentation of the selected eleven stations for the African turbidity network. The location Bilma and some mountains and mountain chains Tassali N'Ajjer (TN), Tibesti (T), Hoggar (H), Air (A), Adrar des Iforhas (AI) and Ennedi (E) are added because of their strategic importance for the dust transport.

### 3. The turbidity network

For the determination of the source strength of pollutants having a surface source such as the Saharan dust, direct or indirect measurements of the aerosol mass load in connection with transport data are needed. The area extension of the Sahara prohibits the use of expensive individual instruments such as lidar or airplane coverage, or the maintenance of a network with time-consuming devices such as a high-volume sampler with additional determination of the collected aerosol mass. Good area coverage is obtained by satellites. Indeed, satellite measurements have been used for desert dust transport studies over the North Atlantic Ocean, for instance, by Carlson and Wendling (1977) and Norton et al. (1980). However, the evaluation of satellite data for turbidity over land surfaces is still inadequate. The reflection properties of land surfaces are anisotropic and the albedo is large and varies strongly with time and location (Koepke et al., 1980). For this reason, a sunphotometer, called "Mainz-sunphotometer," has been developed and proved its suitability and reliability in two years of operation under rough handling and various climatic conditions (d'Almeida et al., 1983).

The following scheme was adapted for estimating the source strength of Saharan dust.

- Development of a sunphotometer to determine the aerosol turbidity.
- Comparison of the sunphotometer with direct aerosol mass samples for "correlating" turbidity with aerosol mass loading.
- Installing and maintaining a network of 11 copies of the Mainz-sunphotometer for more than two years.
- Developing an appropriate transport model to estimate the source strength using the sunphotometer observations and actual meteorological parameters.

Figure 1 gives an overview of the stations selected in Africa for the turbidity network. Reasons for the choice of stations were rather pragmatic but always aimed at the goal of the study.

- A broad coverage of the desert region in order to catch sources not activated simultaneously.
- Relatively close proximity to source areas to observe rather unaged aerosols. Ageing of emitted aerosol leads to a loss of information because the largest particles sediment out rather quickly while smaller ones remain airborne. Therefore, four mandatory "front stations" have been selected. The different transport directions from the sources have been considered.
- The influence of anthropogenic or nonmineral aerosols are unneeded and have to be minimized.
- Some stations are chosen in order to observe the influence of the meridional moving of the ITCZ on the dust transport.
- Simultaneously measured synoptic parameters (wind field, visibility) are desirable for the assessment and an unbiased interpretation of the recorded data.

- Relative easy accessibility of the stations is essential.

The stations Tamanrasset (1380 m) and Assekrem (2730 m), both in Algeria, are about 60 km apart. Tamanrasset observes aerological data. Assekrem has the advantage of being at a higher elevation. Hence, measurements at both stations may give an idea about the height dependence of aerosol and of the trace gases. Both stations are well-situated to monitor the dust transport toward Europe. Boutilimit (Mauritania) is located in the vicinity of source 1 and is therefore suitable for the frequency monitoring of sandstorms in the region. Dakar (Senegal) is not really suitable for a study of background aerosol because of its anthropogenic influence. However, the availability of aerological data supports its choice. The line stretched across Boutilimit (Mauritania), Gao (Mali), Agadez (Niger) and the Wad Medani (Sudan) seizes all activities from the Sahara and the Sahel region and, therefore, enables the investigation of the Saharan dust towards the south. The remaining stations Korhogo (Ivory Coast), Tabligbo close to Lomé (Togo) and Zaria (Nigeria) are influenced by dry and wet depositions and fulfill some of the criteria listed above. Details on the outcome of the African turbidity network are published by d'Almeida (1985).

### 4. Method

#### a. Relation between aerosol turbidity parameters and aerosol mass concentration

The Mainz-sunphotometer was provided with nine interference filters in the spectral range between 400 and 1025 nm. Besides aerosol turbidity parameters, total ozone content (Chappuis-band) and precipitable water ( $\rho\sigma\tau$ -band) are computed using a least-square approximation method for nonlinear equations described by Levenberg (1944), Marquardt (1963) and Brown and Dennis (1972). Total ozone content  $\eta$  and Angström's parameters  $\alpha$  and  $\beta$  have been solved from the following equations:

$$\frac{1}{M} \ln \frac{I_0(\lambda)}{I(\lambda)f} - \tau_R(\lambda) = \beta\lambda^{-\alpha} + \eta a(\lambda)$$

- $M$  relative airmass
- $I_0(\lambda)$  extraterrestrial solar spectral irradiance related to the average distance between earth and sun
- $I(\lambda)$  attenuated incoming solar spectral intensity
- $f$  correction factor for the variable earth-sun distance
- $\tau_R(\lambda)$  Rayleigh scattering coefficient
- $P, P_0$  atmospheric pressures at the station and at sea level
- $\beta$  Angström's turbidity coefficient
- $\alpha$  wavelength exponent
- $a(\lambda)$  ozone absorption coefficient,  $\text{cm}^{-1}$

$\eta$  total ozone content, cm  
 $\lambda$  wavelength.

Methods and results are published by d'Almeida (1983, 1985) and need no special emphasis in this report. We choose  $\beta$ , Angström's turbidity coefficient, to characterize the aerosol extinction feature in the whole spectral range instead of a wavelength-dependent optical depth.  $\beta$  can be correlated with the aerosol mass concentration. The mass concentration  $M$  itself is computable from a known size distribution  $dN(r)$  by integrating the equation

$$dM(r) = \frac{4}{3} \pi r^3 \rho_p dN(r) \quad (1)$$

over the considered size range. Hereby  $\rho_p$  is the particle bulk density in  $\text{g cm}^{-3}$ ,  $dN(r)$  the number concentration in  $\text{cm}^{-3}$  of the particles per radius interval  $r, r + dr$ ,  $dM(r)$  the mass concentration ( $\text{g cm}^{-3}$ ). In that and the following equations the particles are obviously assumed to be spherical. Size distributions measured in the Sahara by d'Almeida and Schütz (1983) during different atmospheric situations are considered in this study. It is shown in that paper that the size spectrum is rather broad and varies between 0.02 and 150  $\mu\text{m}$  radius. Only a part of the particles are, however, optically relevant and detected by a spectral sunphotometer as proved by Mie-computations (Fig. 2). The extinction efficiency  $Q_e[m(\lambda), \lambda, r]$  has been computed for the wavelength 500 nm. The corresponding refractive index has been deduced from measurements carried out by Grams et al. (1974) and Carlson and Caverly (1977). For a polydisperse aerosol the Mie extinction coefficient can be expressed as

$$\sigma_d(m, \lambda) = \int_{r_1}^{r_2} Q_d(m(\lambda), r, \lambda) \pi r^2 \frac{dN(r)}{dr} dr,$$

or

$$\sigma_d(m, \lambda) = \int_{r_1}^{r_2} r^2 \pi \frac{1}{r \ln 10} Q_d(m(\lambda), r, \lambda) \frac{dN(r)}{d \log r} dr. \quad (2)$$

In Fig. 2 the differential extinction coefficient, denoted  $d\sigma_e/d \log r (m, \lambda)$ , and the cumulative extinction coefficient are plotted versus the particle radius  $r$ . The cumulative extinction coefficient is an integration of the differential extinction coefficient over all acting particle radii. Here the cumulative Mie extinction coefficient reveals that 95% of the attenuated solar intensity at 500 nm wavelength are produced by particles smaller than 5  $\mu\text{m}$  in radius.

To express turbidity parameters in terms of airborne aerosol mass concentration, a field campaign was performed in Agadez (Niger) in January and February 1982. The reasons for choosing Agadez as reference station are rather of logistic and pragmatic nature. The station is representative of a large area and is equipped with commercial electric power and running water. Space for careful and sensitive experiments is also available. Furthermore, the dust originating from source 3 needs about two days to reach Agadez. This travel time is obviously long enough to obtain a well-mixed aerosol layer. Some of the instruments used are described by Schütz and Jaenicke (1974) and Jaenicke (1978). Additionally a Winkler-impactor (Winkler, 1975) was modified to collect particles smaller than 5  $\mu\text{m}$  in radius. Collection of the whole suspended aerosol was performed with a high-volume sampler having an average flow rate of  $100 \text{ m}^3 \text{ h}^{-1}$  and an inlet (interchangeable intake cross sections) for guaranteeing a quasi-isokinetic sampling with high collection efficiency for giant particles. For particles smaller than 5  $\mu\text{m}$  radius and a mass concentration range between 30 and  $700 \mu\text{g m}^{-3}$  the following linear relationship is found:

$$C(r \leq 5 \mu\text{m}, \beta) = 404.45\beta + 19.03 \quad (3a)$$

with a correlation coefficient 0.95. Here  $\beta$  is Angström's turbidity coefficient (see Fig. 3) and  $C$  the mass concentration in  $\mu\text{g m}^{-3}$ . A theoretical study developed by Chylek et al. (1979) also yields a linear function between turbidity coefficient and mass concentration and supports our results. Furthermore a mass concentration comparison between the whole suspended particulate matter and particles with radius smaller than 5  $\mu\text{m}$  was performed during the field campaign in Agadez (Fig. 4). The following relationship was found:

$$C(\text{total aerosol}) = 7.8 C(r \leq 5 \mu\text{m}). \quad (3b)$$

It is obvious that Eq. (3b) varies with weather conditions and distance to the source owing to various

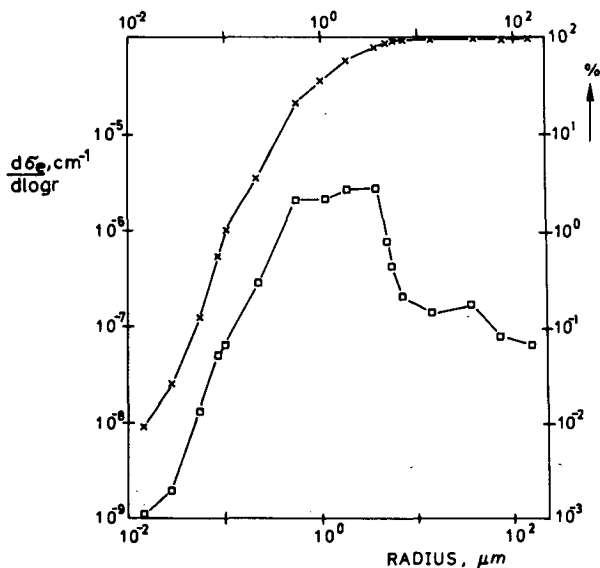


FIG. 2. Differential and cumulative Mie-extinction coefficient.

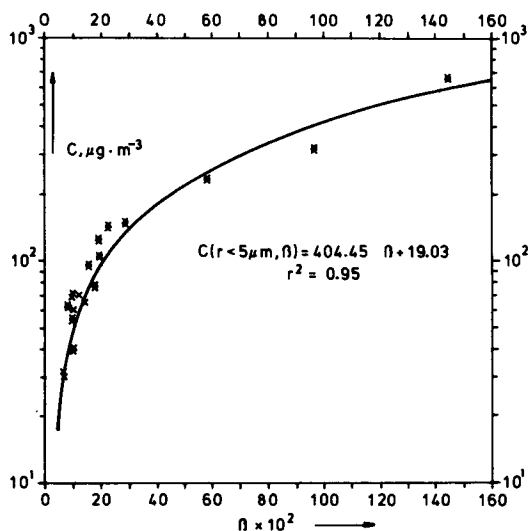


FIG. 3. Mass concentration of mineral dust  $C$ , in  $\mu\text{g m}^{-3}$ , vs Angström turbidity coefficient  $\beta$  in Agadez.

types valid for the source regions can only be found during such critical weather conditions. The variability of the ratio between total mass concentration and long-range transport-related particles during the field campaign in Agadez (Niger) is shown in Fig. 4. The measured mass concentration for total aerosol varied between  $40 \mu\text{g m}^{-3}$  in clear air conditions and  $9300 \mu\text{g m}^{-3}$  during sandstorms (Fig. 4). Compared to the global-average background mass concentration of  $7 \mu\text{g m}^{-3}$  (Heintzenberg, 1980), the Sahara can be seen as a very prominent source of natural aerosol. It is also worth mentioning that a temperature drop up to  $10 \text{ K}$  has been observed during the different duststorm episodes.

Equations (3a) and (3b) warrant an estimation of the mass concentration of airborne particulate matter in terms of an aerosol turbidity parameter. To facilitate matters we assume that these equations are applicable to other source areas although we are well aware of the fact that some differences may occur.

scavenging processes. Keeping in mind that mineral dust is generated by sandstorm or wind carrying dust, it is apparent that a relationship between both particles

*b. Mass balance and model input*

Most of the investigators (e.g., Liu and Seinfeld, 1975; Eliassen, 1980) dealing with the numerical com-

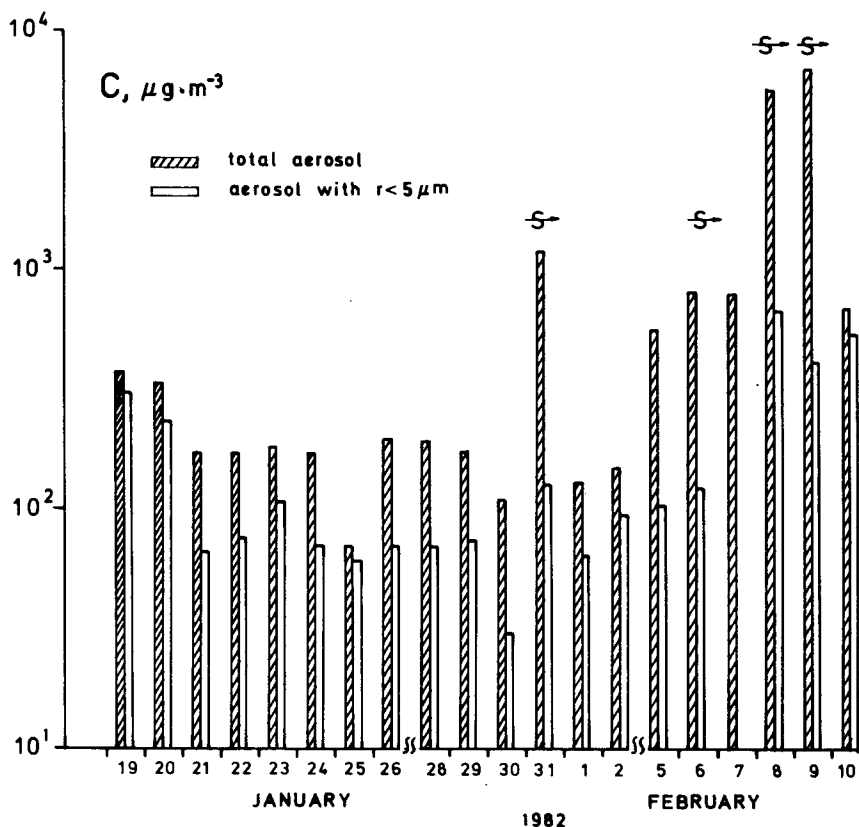


FIG. 4. Mass concentration  $C$ , in  $\mu\text{g m}^{-3}$ , of mineral dust during the field campaign in Agadez (Niger). S means sandstorm episode.

putation of pollutants transport start with the following three-dimensional mass balance equation:

$$\frac{d}{dt}(\rho\bar{\psi}) = \nabla(K \cdot \nabla\rho\bar{\psi}) + Q - R \quad (4)$$

where  $\nabla$  is the Nabla operator,  $\bar{\psi}$  the average mixing ratio of the pollutant per unit mass of air,  $\rho$  the air density,  $K (= K_x, K_y, K_z)$  the eddy-diffusion coefficient,  $Q$  the emission rate or source strength, and  $R$  the removal rate. This equation is often modified and adapted to special problems. In general, models for atmospheric dispersion and transport of pollutants are kinematic models. In such models the air motion is not calculated but taken from meteorological observations and used as model input. The transport of aerosol particles over long distances in the atmosphere is strongly influenced by the time-dependent depth of the layer in which the aerosol is dispersed. This layer, often called the mixing layer, is comparable to the height of the inversion. Sometimes the eddy-diffusion coefficients are taken as constants or empirically related to the height by means of a, more or less, sophisticated parameterization involving the variation of meteorological parameters with altitude (Blakadar, 1962; Liu and Seinfeld, 1975).

Related to the dust transport study in the Sahara, aerological data during noon ascents of Dakar (Senegal), Tamanrasset (Algeria) and Niamey (Niger) have been analyzed in order to determine the vertical extent of dust. The intense insolation beginning early in the morning starts the convection process with the dispersion of the inversion layer and the formation of a mixing height with a quasi-homogeneous aerosol concentration. Therefore, it is apparently difficult to delimit the vertical extent of the Saharan dust by means of conventional aerological soundings as done by Carlson and Prospero (1972) and Schütz (1977). For the model a homogeneous dust layer is assumed and computed using the Mie-theory.

The attenuation of incident monochromatic radiation along its path through the atmosphere due to polydisperse aerosol particles is given by the following equation:

$$\tau_A(\lambda) = \int_H \int_{r_1}^{r_2} \pi r^2 Q_e(m, r, \lambda) \frac{1}{r \ln 10} \frac{dN(r, h)}{d \log r} dr dh, \quad (5)$$

where  $H$  is the height of the homogeneous aerosol layer,  $r$  the radius of the assumed spherical aerosol particles,  $\lambda$  the wavelength of the considered radiation,  $m$  the refractive index of the particles,  $Q_e$  the kernel or Mie-extinction efficiency for the wavelength 500 nm, and  $r_1$  and  $r_2$  are given by the differential distribution of the Mie coefficient, with  $r_1 = 0.1$  and  $r_2 = 5 \mu\text{m}$  (Fig. 2).  $\tau_A(\lambda)$  is the aerosol optical depth as measured with a spectral sunphotometer. We choose the wavelength 500 nm to compute  $H$  from Eq. 5 since the refractive

index for mineral particles is known and optical depth measurements is made for that wavelength.

$$H = \frac{\tau_A(\lambda)}{\int_{r_1}^{r_2} \pi r^2 \frac{1}{r \ln 10} Q_e(m, r, \lambda) \frac{dN(r, h = h_0)}{d \log r} dr} \quad (6)$$

Figure 5 shows computed monthly average values of the dust-layer height for four stations of the turbidity network. The values vary between some 200 m in winter for the mountain station Assekrem (2730 m, Algeria) and some 3000 m in warm season for a front-station like Agadez (Niger).

There are some gaps in the sunphotometer data recording due either to instrument damage or inadequate weather conditions. Horizontal visibility and aerosol turbidity parameters are often related to each other. We use this facility to obtain a coherent pattern of the turbidity variation. A correlation analysis between horizontal visibility  $VV$  and  $\beta$  has then been achieved and results in the following empirical formula:

$$\beta = 2.26 VV^{-0.73} \quad (7)$$

Most of the data used originated from Assekrem (2730 m, Algeria), where the visibility range varies between 400 km in winter and 3 km in summer. The remaining data came from Boutilimit (Mauritania), a station with a maximum probability of dust occurrence. A combination of Eq. (3a) and Eq. (7) yields the following relationship for particles with radius smaller than  $5 \mu\text{m}$

$$C = 914.06 VV^{-0.73} + 19.03 \quad (8)$$

This equation permits the horizontal visibility  $VV$  in km to be expressed in terms of aerosol mass concentration  $C$  in  $\mu\text{g m}^{-3}$  and vice versa. Extrapolating Eq. (8) for sandstorms which involve particles up to 100  $\mu\text{m}$  radius and a visibility down to 100 m leads to a mass concentration of about  $38 \text{ mg m}^{-3}$  for all suspended particulate matter. Compared to the extreme value, reported by Orgill and Sehmel (1976), of  $176 \text{ mg m}^{-3}$ , our value seems to be realistic.

In Fig. 7 the monthly average values of  $\beta$  are plotted as function of time for some selected stations. As can be seen the turbidity values peak between March and June for all stations. That period corresponds to the sunniest and highest temperature and the lowest rainfall intensity (Griffiths, 1972). High insolation seems to match with high turbidity. The station Wad Medani (Sudan) does not show a seasonal turbidity variation. It is not clear if the dust activity was confined in another area or less pronounced during the two monitoring years.

The simplifications we state by assuming a layer with homogeneous dust concentration make the  $K$ -coefficients unnecessary in Eq. (4). Additionally, steady state

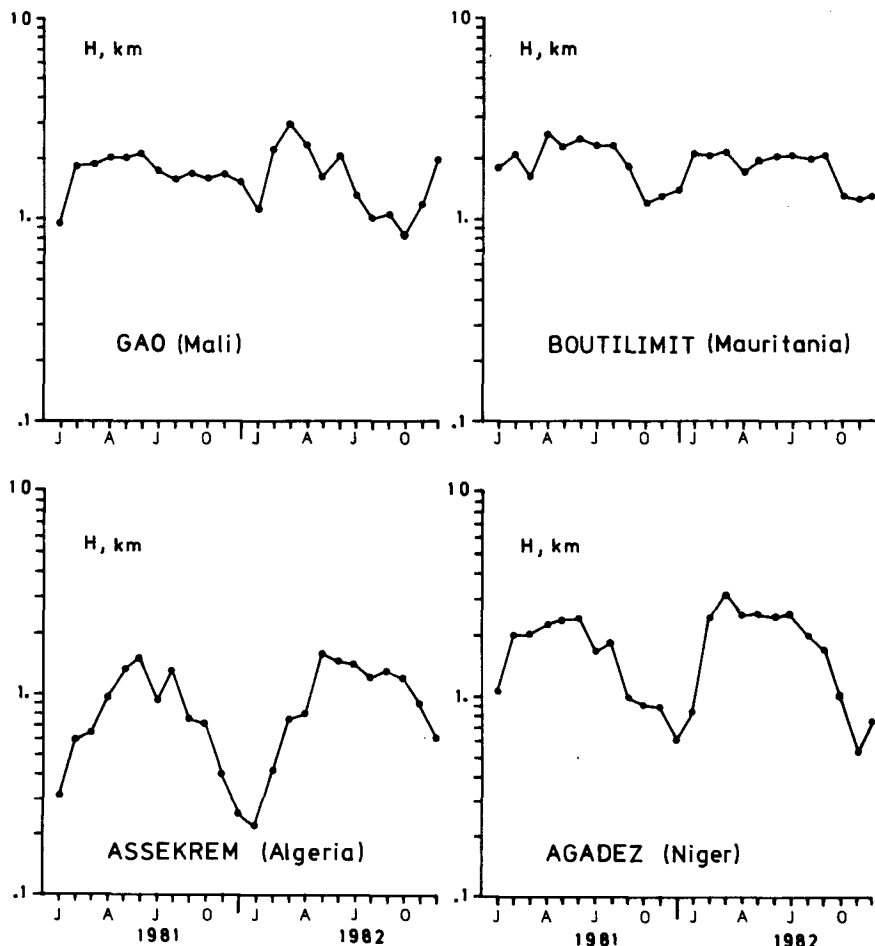


FIG. 5. Monthly average values of homogenous aerosol layer height.

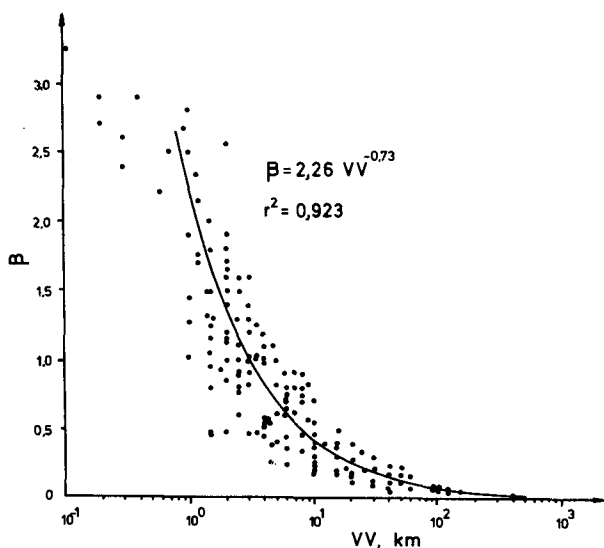


FIG. 6. Plot of Angström turbidity coefficient  $\beta$  vs estimated visibility VV in km.

conditions are considered. The mean mixing ratio is expressed in terms of the mean concentration. Computation of the source strength is performed using a box model. The model takes into account the seasonal migration of the ITCZ described by Griffiths (1972), Dhonneur (1974), Newell and Kidson (1979). Information about the daily variation of the actual wind field between source and sink regions is obtained from the regional meteorological stations. As scavenging processes, dry deposition (absorption or retention at the surface) and wet deposition (removal by rain) are considered. Dimensions of the source areas are obtained through planimetry. Secondary source regions are not considered. Resuspension of particles between sources and sinks is not permitted, and any changes in chemical composition during transport are ignored. Also scavenging by thermophoresis and diffusiophoresis is not considered. Equation (4) then becomes

$$U(x, z) \frac{\partial C(x)}{\partial x} = Q - R. \tag{9}$$

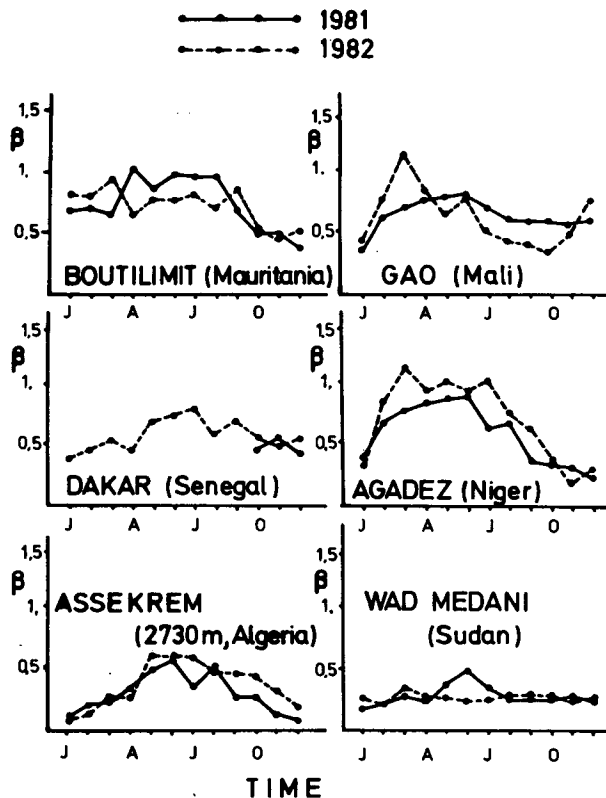


FIG. 7. Monthly average values of Angström turbidity coefficient for some selected stations of the African turbidity network.

As indicated above  $Q - R = R_D + R_W$ . The quantities  $R_D$  and  $R_W$  mean the dry and wet depositions. The  $z$ -dependence of the wind speed is eliminated by using the relationship,

$$\bar{U}(x) = \frac{1}{H} \int_0^H U(x, z) dz. \quad (10)$$

Scavenging processes for removing aerosols and some trace gases from the atmosphere have been discussed by many investigators (Rodhe and Grandell, 1972; Shepherd, 1974; Whelpdale and Shaw, 1974; Dovland and Eliassen, 1976). The dry deposition at a distance  $x$  from the source is given by

$$R_D = (\epsilon + D) \frac{dC}{dz} + \frac{v_t C}{H} \quad (11)$$

where  $\epsilon$  and  $D$  are the turbulent diffusion coefficient and the Brownian diffusion coefficient and  $v_t$ , the deposition velocity of the particles. With the preceding assumptions the first term of the right hand of Eq. (11) can be ignored. The deposition velocity varies with particles dimension. A subdivision of the aerosol size spectrum in small intervals is therefore necessary for its computation. The  $v_t$  can be derived from the Langevin's equation by suppressing electrostatic forces. For submicroscopic particles the slip-flow Cunningham

correction  $(1 + Z_t N_{kn})$  is incorporated. The correction factor increases the sedimentation velocity of about 16% for particles with  $1 \mu\text{m}$  radius and standard conditions. For spherical particles with a bulk density  $\rho_p = 2.5 \text{ g cm}^{-3}$ ,  $v_t$  may be obtained from the following expression:

$$\dot{V}_t = \frac{2(1 + Z_t N_{kn}) r^2 g (\rho_p - \rho)}{9\eta} \quad (12)$$

with

- $Z_t$  1.257 + 0.4 exp(-1.1/ $N_{kn}$ ) after Pruppacher and Klett (1978),
- $N_{kn}$  Knudson's number,
- $\rho$  density of air,
- $g$  acceleration of gravity,
- $\eta$  dynamic viscosity of air.

Wet deposition is the second scavenging process we consider. It is often separated into "rainout" (the incorporation of particles or gases into cloud droplets within the cloud) and "washout" (removal through falling precipitation elements below the cloud). The different theoretical formulations of authors dealing with this problem (Junge, 1963; Scriven and Fisher, 1975; McMahon et al., 1976) show that the handling of processes leading to wet deposition is not entirely understood. However, it is obvious that wet deposition is characterized by a washout coefficient  $\Lambda$ , called Langmuir's factor, which gives the fraction of effluent removed per unit time. The wet deposition rate can then be expressed as

$$R = \Lambda f^* C \quad (13)$$

where  $f^*$  is the fraction of the distance  $x$  over which rain is falling at the rate specified by the quantity  $\Lambda$ . A theoretical study reported by Chamberlain (1955) gives the value  $\Lambda = 3 \times 10^5 J_w$  per  $s$  for the washout coefficient. Hereby  $J_w$  is the rainfall intensity in  $\text{mm h}^{-1}$ , a function of the transport distance  $x$ .

Figure 8 represents the box model used to compute the source strength and deposition rate in which  $l_0$  and  $L$  specify the length and the width of the source area considered. It is assumed that the effluent crosses some vertical plane with uniform concentration  $C(x)$  and a height  $H$  corresponding to the vertical extent of the dust. The actual average wind field between the Earth's surface and 700 mb is considered for this analysis (see Eq. 10). An angle of dispersion of 45 deg on both sides of the transport direction leads to the following classification. The wind field varying between

- 340 and 70 deg is considered as the south transport (transport towards the Gulf of Guinea)
- 70 and 160 deg results in the west transport (transport over the northern equatorial Atlantic)
- 160 and 250 deg forms the north transport (transport to Europe)
- 250 and 340 deg is called the east transport.



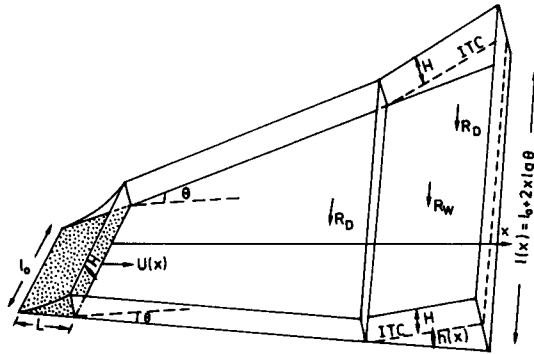


FIG. 8. Box model for the computation of the source strength and deposition rate of Saharan dust. Dust is emerging from the source (dotted field). Owing to convective processes and wind-shear turbulence, the dust is diffused upward to higher altitudes where the wind is strong enough for further transportation in the horizontal direction. An angle of dispersion of 45 deg on both sides of the transport direction is permitted for the classification of the wind field in four quadrants.  $H$ : homogenous dust layer height;  $l_0$  and  $L$ : the length and the width of the source areas.

The wind data originated from actual observations of the different regional meteorological stations. In addition "European Meteorological Bulletins" are used to follow the north transport.

After a given time  $x/U(x)$  the remaining effluent crosses a vertical plane with a distance  $x$  from the source and a height  $H_0(x) = H + h(x)$  and a width  $l(x) = l_0 + 2x \tan \theta = l_0 + 2x$ . Here  $h(x)$  is the variable height of the monsoon layer (see Fig. 8). North of the monsoon layer only dry deposition takes place. In the monsoon layer both dry and wet deposition occur. The monthly average rainfall  $J_w$  as function of the distance from the source is computed for 43 stations within the latitudes and longitudes considered. The data are based on 10 to 50 yr rainfall observations tabulated by Griffiths (1972). The emission strength of the four identified sources (Fig. 2) is computed from the turbidity data of the four front stations—Boutilimit (Mauritania), Gao (Mali), Agadez (Niger) and Wad Medani (Sudan)—by taking into account Eq. (3b). The source strength  $Q(x)$  at a distance  $x$  from the source can be expressed by the following equation:

$$Q(x) = 7.8C(\beta)(l_0 + 2x) \frac{L_0 H(x)}{2F} \quad (14)$$

where the mass concentration  $C(\beta)$  in  $\mu\text{g m}^{-3}$  expressed as function of aerosol turbidity parameter is given by Eqs. (3a) and (3b) and  $F$  denotes frequency of the dust transport in a given direction per unit time. Considering Eqs. (9)–(14) and the simplifications stated before, the following equation can be obtained:

$$Q(x=0) = Q(x_{\text{front}}) \exp \left[ \int_{x=0}^{x_{\text{front}}} \frac{1}{U(x)} \left( \frac{v_t}{H(x)} + f^* q J_w(x) \right) dx \right] \quad (15)$$

where  $q$  is a correction factor for unit and  $x_{\text{front}}$  means the distance between the front stations Boutilimit, Gao, Agadez or Wad Medani and their respective source regions.  $Q(x=0)$  and  $Q(x_{\text{front}})$  express production at the source regions and at the front stations. This model gives computed source strength and deposition rate on a monthly basis.

5. Results

Figure 9 and Tables 1a and 1b give an overview of the computed source strengths of the different source areas as functions of time and the transport direction for the two monitoring years 1981 and 1982. It is noteworthy that dust transport takes place throughout the year but is particularly strengthened between March and June. The transport direction is determined by the general circulation pattern.

The dust plume spreading towards the Sahel region and the Gulf of Guinea originates from all four source regions and is of frequent occurrence in wintertime. The prevailing wind field promotes its propagation. The source region in the lowland north and northeast of Dirku (Niger) and Faya Largeau produces propor-

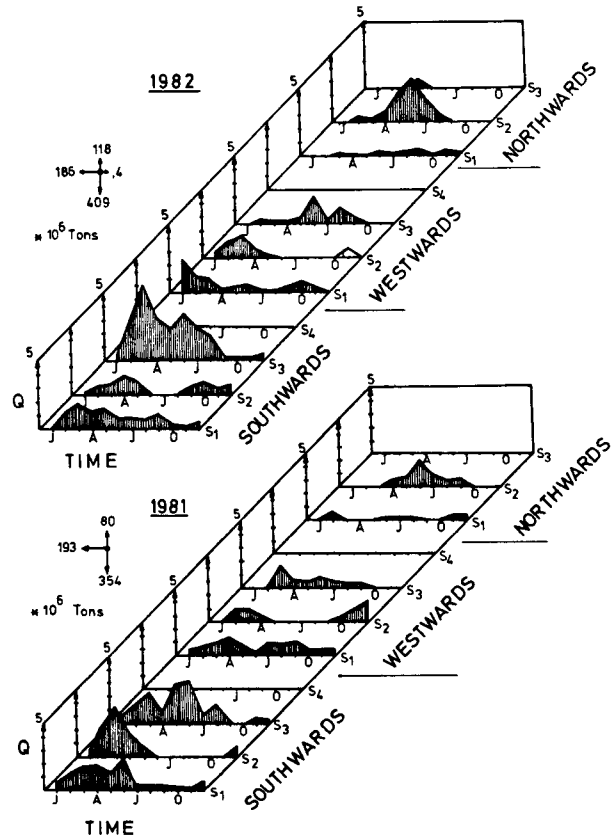


FIG. 9. Computed source strength in  $10^6 \text{ t mo}^{-1}$  for the different source areas as function of time.  $S_1, S_2, S_3$  and  $S_4$  are the different source areas of Fig. 2.

TABLE 1a. Dust production in the different directions (westward ←, southward ↓, northward ↑) computed for January (Jan) to December (Dec) 1981. The total monthly and annual amounts are also given.

1981	Source region				Σ
	1	2	3	4	
Jan	4.8 ← ↑1.2 ↓6.04	1.2 ← ↑6.5 ↓	0.03 ← ↑6.1 ↓	0.2 ← ↑0.05 ↓	6.2 ← ↑1.2 ↓18.7
Feb	7.0 ← ↑6.9 ↓13.9	9.2 ← ↑15.9 ↓	0.3 ← ↑15.0 ↓	↓0.4	16.5 ← ↑6.9 ↓42.2
Mar	9.2 ← ↑18.3 ↓	9.7 ← ↑38.5 ↓	↓23.2	↓0.1	18.9 ← ↑80.1 ↓
Apr	14.2 ← ↑18.9 ↓	5.6 ← ↑5.1 ↓17.5	16.9 ← ↑0.2 ↓10.7	0.12 ← ↑0.12 ↓0.24	36.8 ← ↑5.4 ↓47.3
May	8.04 ← ↑13.4 ↓	0.3 ← ↑6.9 ↓8.2	6.2 ← ↑0.3 ↓24.0	0.06 ← ↑0.1 ↓0.06	14.6 ← ↑7.3 ↓45.7
Jun	2.04 ← ↑2.04 ↓25.0	0.4 ← ↑20.9 ↓0.2	5.1 ← ↑26.8 ↓	0.7 ← ↑3.0 ↓	8.2 ← ↑25.9 ↓52
Jul	9.5 ← ↑2.4 ↓4.8	0.1 ← ↑8.8 ↓0.08	8.5 ← ↑6.8 ↓	0.3 ← ↑0.3 ↓	18.5 ← ↑11.5 ↓11.7
Aug	8.4 ← ↑2.1 ↓4.2	0.6 ← ↑4.5 ↓1.4	4.7 ← ↑0.2 ↓14.0	↓0.2 ↑0.04	13.7 ← ↑7 ↓19.6
Sep	11.1 ← ↑3.7 ↓	0.4 ← ↑5.5 ↓0.7	4.1 ← ↑0.3 ↓0.9	0.05 ← ↑0.3 ↓0.1	15.7 ← ↑6.1 ↓5.4
Oct	4.0 ← ↑2.0 ↓	3.5 ← ↑0.6 ↓0.4	3.7 ← ↑1.1 ↓	0.2 ← ↑0.3 ↓	11.4 ← ↑0.6 ↓3.8
Nov	3.9 ← ↑3.8 ↓1.5	8.5 ← ↑0.5 ↓	0.1 ← ↑4.0 ↓	0.05 ← ↑0.2 ↓1.5	12.6 ← ↑4 ↓7.5
Dec	4.3 ← ↑4.4 ↓7.3	15.2 ← ↑6.9 ↓	0.2 ← ↑2.0 ↓	↓1.1	19.8 ← ↑4.4 ↓17.3
Σ: 193 ← ↑80 ↓354	86.5 ← ↑22.8 ↓119.0	54.7 ← ↑52.3 ↓96.8	49.8 ← ↑1.0 ↓134.6	1.5 ← ↑4.2 ↓3.9	

tionally the greatest part of the dust transported southward. The dust production in summer is nearly scavenged by the monsoon air mass with its high water vapor content. The region south of the ITCZ is, therefore, shielded in this season from dust loaded winds coming from the Sahara. The contribution of source 4 is relatively small. It remains uncertain if Wad Medani is appropriate enough as a front station or if the dust is confined elsewhere or if that source was not productive during the monitoring years.

As for the source strength towards the Gulf of Guinea, an amount of about  $350 \times 10^6$  and  $410 \times 10^6$

$t \text{ yr}^{-1}$  for all suspended particulate matter and about  $45 \times 10^6$  and  $53 \times 10^6 t \text{ yr}^{-1}$  for long-range transport-related aerosol particles has been computed for the years 1981 and 1982, respectively. These results are thought to be the first estimation of the south transport so far.

The west-transport also occurs throughout the year. The main portion is produced by source 1 (Fig. 1). For the monitoring years 1981 and 1982 about  $190 \times 10^6 t$  for all particles and  $24 \times 10^6 t$  for long-range transport-related particles have been emitted each year towards the equatorial North Atlantic and towards the Antilles.

TABLE 1b. Dust production in the different directions (westwards ←, southwards ↓, northwards ↑) computed for January (Jan) to December (Dec) 1982. The total monthly and annual amounts are also given.

1982	1	2	3	4	Σ
Jan	24.5 ← <sup>0.7</sup> ↓	4.5 ← ↓ <sup>1.8</sup>	0.2 ← ↓ <sup>3.8</sup>	0.2 ← ↓ <sup>0.8</sup>	29.4 ← <sup>0.7</sup> ↓ <sup>6.4</sup>
Feb	12.3 ← ↓ <sup>13.0</sup>	13.6 ← ↓ <sup>6.7</sup>	2.1 ← ↓ <sup>29.2</sup>	0.04 ↓ ↑ <sup>0.6</sup>	28 ← <sup>0.04</sup> ↓ <sup>49.5</sup>
Mar	10.0 ← <sup>2.0</sup> ↓ <sup>19.4</sup>	17.1 ← <sup>3.9</sup> ↓ <sup>8.8</sup> 0.4	2.2 ← ↓ <sup>55.4</sup>	0.08 ↓ ↑ <sup>0.8</sup>	29.3 ← <sup>6</sup> ↓ <sup>84.4</sup> 0.4
Apr	2.4 ← <sup>0.8</sup> ↓ <sup>13.2</sup>	7.7 ← <sup>1.8</sup> ↓ <sup>15.5</sup>	1.2 ← ↓ <sup>29.9</sup>	0.1 ↓ ↑ <sup>0.1</sup>	11.3 ← <sup>2.7</sup> ↓ <sup>58.7</sup>
May	4.4 ← <sup>0.1</sup> ↓ <sup>16.3</sup>	2.5 ← <sup>6.6</sup> ↓ <sup>10.1</sup>	3.2 ← ↓ <sup>23.5</sup>	0.2 ← <sup>0.2</sup> ↓ <sup>0.5</sup>	10.3 ← <sup>6.9</sup> ↓ <sup>50.4</sup>
Jun	6.0 ← <sup>2.5</sup> ↓ <sup>7.9</sup>	0.4 ← <sup>21.0</sup> ↓ <sup>0.2</sup>	20.2 ← ↓ <sup>33.6</sup>	0.1 ← <sup>0.2</sup> ↓ <sup>0.5</sup>	26.7 ← <sup>23.7</sup> ↓ <sup>42.2</sup>
Jul	1.0 ← <sup>1.4</sup> ↓ <sup>8.4</sup>	0.04 ← <sup>31.5</sup> ↓ <sup>0.1</sup>	0.3 ← ↓ <sup>23.8</sup>	0.2 ↑	1.34 ← <sup>33.1</sup> ↓ <sup>32.3</sup>
Aug	0.8 ← <sup>2.9</sup> ↓ <sup>7.0</sup>	0.2 ← <sup>17.3</sup> ↓ <sup>0.6</sup>	4.4 ← <sup>7.3</sup> ↓ <sup>17.5</sup>	0.3 ← <sup>0.2</sup> ↓ <sup>0.7</sup>	5.7 ← <sup>27.7</sup> ↓ <sup>25.8</sup>
Sep	4.2 ← <sup>4.9</sup> ↓ <sup>11.4</sup>	0.9 ← <sup>4.2</sup> ↓ <sup>6.5</sup>	12.2 ← <sup>0.8</sup> ↓ <sup>2.7</sup>	0.1 ← <sup>0.1</sup> ↓ <sup>0.5</sup>	17.4 ← <sup>10.1</sup> ↓ <sup>21.1</sup>
Oct	7.2 ← ↓ <sup>3.6</sup>	↓ <sup>9.9</sup>	4.9 ← ↓ <sup>1.6</sup>	0.4 ← <sup>0.3</sup> ↓ <sup>0.4</sup>	12.5 ← <sup>0.3</sup> ↓ <sup>15.5</sup>
Nov	3.6 ← <sup>3.6</sup> ↓ <sup>1.4</sup>	6.1 ← <sup>0.2</sup> ↓ <sup>3.8</sup>	0.1 ← ↓ <sup>1.4</sup>	0.1 ← ↓ <sup>0.4</sup>	9.9 ← <sup>3.8</sup> ↓ <sup>7</sup>
Dec	2.8 ← <sup>2.8</sup> ↓ <sup>4.6</sup>	0.6 ← ↓ <sup>7.2</sup>	0.3 ← ↓ <sup>3.1</sup>	0.1 ← ↓ <sup>0.8</sup>	3.8 ← <sup>2.8</sup> ↓ <sup>15.7</sup>
Σ: 186 ← <sup>118</sup> ↓ <sup>409</sup>	79.2 ← <sup>21.7</sup> ↓ <sup>106.2</sup>	53.6 ← <sup>86.5</sup> ↓ <sup>71.2</sup> 0.4	51.3 ← <sup>8.1</sup> ↓ <sup>225.5</sup>	1.5 ← <sup>1.4</sup> ↓ <sup>6.1</sup>	

Earlier investigations of Carlson and Prospero (1972), Prospero and Carlson (1972) and Schütz (1977) led to results showing some differences (Table 2). These differences may be attributable to two reasons:

(i) annual variations in the source strength may happen in spite of the fact that the present study gives similar results for 1981 and 1982.

(ii) the different reference locations from which observations have been made. The aerosol properties alter with the residence time and the travel distance.

Saharan dust transport to Europe is both less pro-

nounced and of rather sporadic nature. It often occurs in summer months and mainly originates from source 2 (Fig. 1). However, the contribution of source 1 is not negligible. For 1981 and 1982,  $80 \times 10^6$  and  $120 \times 10^6$  t for all particles and about  $10 \times 10^6$  and  $16 \times 10^6$  t for particles smaller than  $5 \mu\text{m}$  radius were delivered from the Sahara, respectively. The source strength toward Europe had also never been estimated before.

The general circulation over the Sahara prevents the eastward transport that only occurs occasionally. The model shows such a case for March 1982 for which only a negligible quantity of about  $0.4 \times 10^6$  t has been computed.

An important part of the dust emerging from the source areas remains on the continent after being scavenged. Another part leads to the formation of deep-sea sediments. Figure 10 illustrates the amount of dust deposition in the Atlantic. For the south transport and the production areas 2 and 3, the amount of dust reaching the  $5^{\circ}$  N latitude (Gulf of Guinea) is of about  $5 \times 10^6$  t yr $^{-1}$ . Most of the dust emitted southward is scavenged on the continent and might affect farm lands and the agriculture of this region since the Saharan dust contains numerous mineral nutrients (Domergue, 1980). The dust deposit may probably also contribute to the desert extension, hence to the desertification. On the other hand nearly 75% of the dust emitted westward contributes to the formation of deep-sea sediments in the equatorial North Atlantic. The amount of dust deposit in the Mediterranean could not be investigated because of lack of reliable data.

The drought (rainfall deficit) of recent years does not considerably affect the evaluation of source strength because between front stations and source regions the scavenging process is mostly limited to dry deposition. As it can be deduced from the present report, the emphasis of this investigation is basically to compute the source strength of Saharan dust in the different directions. The two monitoring-years do not allow one to draw conclusions on the impact of the recent drought. Neither is it possible to stress the importance of the subsequent rainfall deficits. A more extended monitoring activity is needed for a reliable statement. That can hardly be expected in the framework of a one-man university research activity.

## 6. Conclusions

The present study reveals the Saharan desert as an important source for mineral dust influencing the North Atlantic Ocean, Europe to a lesser extent, and, to a large extent, the precipitation zone of the ITCZ. If the amount of mineral dust released from the Sahara is extrapolated to all deserts of the world, i.e., if we assumed the production per unit area to be the same, global mineral source strength of some 1900 million tons and 240 million tons per year for all aerosol par-

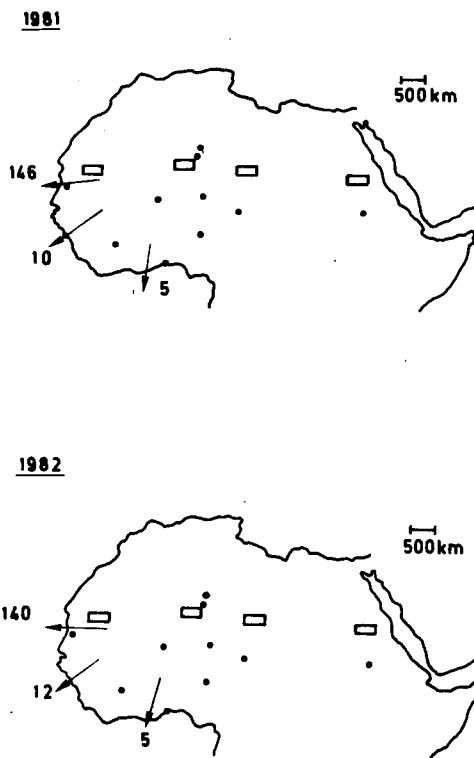


FIG. 10. On the sedimentation rate of Saharan dust in  $10^6$  t yr $^{-1}$  as computed by the model. The small rectangles are a tentative representation of the source areas and the dots mean the stations of the African turbidity network.

ticles and for long-range transport related particles result, respectively. This study illustrates that the contribution and importance of mineral dust to the total burden of tropospheric aerosols have been underestimated so far. From this point of view the results might be useful for further computation of radiative heating or cooling rates, for a world wide aerosol climatology and for new designed long-term climate models. Furthermore, the results of this monitoring program for mineral dust might serve as a reference point, if future studies focus on the variability of such sources, or on secular trends with its impact on the regional and global climate.

*Acknowledgments.* The present work was carried out in the "Sonderforschungsbereich: Trace Substances of the Atmosphere," sponsored by the German Science Foundation (DFG) when the author was with the University of Mainz. The field experiments in Agadez were supported by the Government of the Republic Niger. Sunphotometer observations were only possible with the technical help of Mr. A. Köhler, Chief, Environment Division, World Meteorological Organization (WMO) in Geneva and the different national meteorological office headquarters. The author is grateful to

TABLE 2. Results comparison of the westward component of Saharan dust transport.

Author	Monitoring location	Source strength (west-component) ( $10^6$ t/yr $^{-1}$ )
Carlson and Prospero (1972)	Barbados	80
Schütz (1977)	Cape Verde Islands	260
Present report	Vicinity of the source regions in the Sahara	190

all observers, particularly to Frère Jean Marie Cortade in the hermitage of Assekrem (Algeria), to Drs. A. Ben Mohamed and J. L. Domergue of University of Niamey (Niger) for their kind assistance, to Dr. A. E. Kalu of the Research and Training Center in Lagos (Nigeria) and to all observers in the different stations, for the substantial discussions and the exemplary co-operation. The author wishes to thank Prof. Dr. R. Jaenicke and Dr. L. Schütz of University of Mainz (F.R.G.) for their considerable suggestions, support and helpful advice.

## REFERENCES

- Bertrand, J., J. Baudet and A. Drochon, 1974: Importance des aérosols naturels en Afrique de l'ouest. *J. Rech. Atmos.*, **8**, 846–860.
- Blakadar, A. K., 1962: The vertical distribution of wind and turbulent exchange in a neutral atmosphere. *J. Geophys. Res.*, **67**, 3095–3102.
- Brown, K. W., and J. E. Dennis, Jr., 1972: Derivative free analogues of Levenberg-Marquardt and Gauss algorithms for nonlinear least square approximation. *Numer. Math.*, **18**, 289–297.
- Carlson, T. N., and J. M. Prospero, 1972: The large scale movement of Saharan air outbreaks over the equatorial North Atlantic. *J. Appl. Meteor.*, **11**, 289–297.
- , and R. S. Caverly, 1977: Radiative characteristics of Saharan dust at solar wavelengths. *J. Geophys. Res.*, **82**, 3141–3152.
- , and P. Wendling, 1977: Reflected radiance measured by NOAA and VHR as a function of optical depth for Sahara dust. *J. Appl. Meteor.*, **16**, 1368–1371.
- Chamberlain, A. C., 1955: Aspects of travel and deposition of aerosol and vapor clouds. A.E.R.E. HP/R, 1261 pp.
- Chylek, P., J. T. Kiehl and M. K. W. Ko, 1979: Infrared extinction and the mass concentration of atmospheric aerosols. *Atmos. Environ.*, **13**, 169–173.
- D'Almeida, G. A., 1979: Die vollständige mineralische Größenverteilung und Diskussion möglicher Quellgebiete von Sandstürmen der zentralen westlichen und südwestlichen Sahara. Wissenschaftliche Mitteilung. Johannes Gutenberg Universität, Inst. f. Meteorologie, Mainz, F.R.G. 101 pp.
- , 1983: Der Staubtransport aus der Sahara. Ph.D. thesis, University of Mainz, F.R.G., 171 pp.
- , 1985: Recommendation on sunphotometer measurements in the BAPMON as based on the experiment of a dust transport study in Africa. WMO/TD-67, WMO, 30 pp.
- , and L. Schütz, 1983: Number, mass and volume distribution of mineral aerosol and soils of the Sahara. *J. Climate Appl. Meteor.*, **22**, 233–243.
- , R. Jaenicke, R. Roggendorf and D. Richter, 1983: New sunphotometer for network operation. *Appl. Opt.*, **22**, 3796–3801.
- DeLuisi, J. J., I. H. Blifford, Jr. and J. A. Takamine, 1972: Models of tropospheric aerosol size distribution derived from measurements at three locations. *J. Geophys. Res.*, **20**, 4529–4538.
- Dhonneur, G., 1974: Nouvelle approche des réalités Météorologiques de l'Afrique occidentale et centrale. Thèse présentée pour l'obtention du diplôme de docteur ingénieur No. d'ordre 3, publication de l'ASECNA, Tomes I et II, 1–351 et 1–472.
- Domergue, J. L., 1980: Contribution à l'étude des aérosols atmosphériques d'origine naturelle en Afrique de l'ouest. Thèse de doctorat de sciences physiques, Université Paul Sabatier, Toulouse, France, 165 pp.
- Dovland, H., and A. Eliassen, 1976: Dry deposition on a snow surface. *Atmos Environ.*, **10**, 783–785.
- Dubief, J., 1979: Review of the North African climate with particular emphasis on the production of eolian dust in the Sahel Zone and in the Sahara. *Saharan Dust: Mobilization, Transport, Deposition*, C. Morales, Ed., Wiley & Sons, 27–48.
- Eliassen, A., 1980: A review of long-range transport modeling. *J. Appl. Meteor.*, **19**, 231–240.
- Grams, G. W., I. H. Blifford Jr., D. A. Gillette and P. B. Russel, 1974: Complex index of refraction of airborne particles. *J. Appl. Meteor.*, **13**, 459–471.
- Griffiths, J. F., 1972: *World Survey of Climatology—Climates of Africa*. Landsberg, Ed. in chief, Elsevier, 604 pp.
- Hänel, G., and K. Bullrich, 1978: Physico-chemical property models of tropospheric aerosol particles. *Beitr. Phys. Atmos.*, **51**, 129–138.
- Heintzenberg, J., 1980: Particle size distribution and optical properties of arctic haze. *Tellus*, **32**, 251–260.
- Jaenicke, R., 1978: Aitken particle size distribution in the Atlantic North East trade wind. "Meteor" *Forschungsergeb. Reihe B*: **7**, 1–21.
- , and L. Schütz, 1978: Comprehensive study of physical and chemical properties of the surface aerosol in the Cape Verde Island regions. *J. Geophys. Res.*, **83**, 3583–3599.
- , 1980: Natural aerosols. *Ann. NY Acad. Sci.* **338**, 317–329.
- Joseph, J. H., A. Manes and D. Ashbel, 1973: Desert aerosols transported by Khamsinic and their climatic effects. *J. Appl. Meteor.*, **12**, 792–797.
- Junge, Ch. E., 1963: *Air Chemistry and Radioactivity*. Academic Press, 382 pp.
- Kalu, A. E., 1979: The African dust plume: Its characteristics and propagation across West Africa in winter. *Saharan Dust: Mobilization, Transport, Deposition*, C. Morales, Ed., Wiley & Sons, 95–118.
- Koepke, P., H. Quenzel and M. Kaestner, 1980: Monitoring of atmospheric turbidity from geostationary satellites. Paper presented at WMO Tech. Conf. on Regional and Global Observation of Atmospheric Pollution Relative to Climate, Boulder, CO, WMO No 529, 49–56.
- Lenoble, J., and C. Brogniez, 1984: A comparative review of radiation aerosol models. *Beit. Phys. Atmosph.*, **57**, 1–20.
- Levenberg, K., 1944: A method for the solution of certain nonlinear problems in least squares. *Quart. Appl. Math.*, **2**, 164–168.
- Liu, M. K., and J. H. Seinfeld, 1975: On the validity of grid and trajectory models of urban air pollution. *Atmos. Environ.*, **9**, 555–574.
- McMahon, T. A., P. J. Denison and R. Fleming, 1976: A long-distance air pollution transportation model incorporating washout and dry deposition components. *Atmos. Environ.*, **10**, 751–761.
- Marquardt, D. W., 1963: An algorithm for least square estimation of nonlinear parameters. *J. SIAM*, **11**, 431–441.
- Meigs, R., 1953: World distribution of arid and semi-arid climates in review of research on arid zone hydrology: *UNESCO, Pans. Arid Zone Programs*, **1**, 203–210.
- Morales, C., Ed., 1979: *Saharan Dust: Mobilization, Transport, Deposition*. Wiley & Sons.
- , 1981: A case study of a dust storm weather situation in the Sudan in April 1973. *Pure Appl. Geophys.*, **19**, 658–676.
- Newell, R. E., and J. W. Kidson, 1979: The tropospheric circulation. *Saharan Dust: Mobilization, Transport, Deposition*. C. Morales, Ed., Wiley & Sons, 133–169.
- Orgill, M. M., and G. A. Sehmel, 1976: Frequency and rupture variation of dust storms in the contiguous USA. *Atmos. Environ.*, **10**, 813–825.
- Patterson, E. M., D. A. Gillette and B. H. Stockton, 1977: Complex index of refraction between 300 nm and 700 nm for Saharan aerosols. *J. Geophys. Res.*, **82**, 3153–3160.
- Peterson, S. T., and C. E. Junge, 1971: Sources of particulate matter in the atmosphere. *Man's Impact on the Climate*. W. W. Kellogg and G. D. Robinson, Eds., MIT Press, 310–320.
- Prospero, J. M., and T. N. Carlson, 1972: Dust concentration in the atmosphere of the equatorial North Atlantic Ocean. *J. Geophys. Res.*, **77**, 5255–5265.
- Pruppacher, H. R., and J. D. Klett, 1978: *Microphysics of Clouds and Precipitation*. Reidel, 714 pp.

- Schütz, L., 1977: Die Saharastaubkomponente über dem subtropischen Nord-atlantik. Ph.D. thesis, Universität Mainz, 155 pp.
- , and R. Jaenicke, 1974: Particle number and mass distribution above  $10^{-4}$  cm radius in sand and aerosol of the Sahara Desert. *J. Appl. Meteor.*, **13**, 863–870.
- Scriven, R. A., and B. E. Fisher, 1975: The long-range transport of airborne material and its removal by deposition and washout, I, General Considerations. *Atmos. Environ.*, **9**, 49–58.
- Shepherd, J. G., 1974: Measurements of the direct deposition of sulphure dioxide onto grass and water by the profile method. *Atmos. Environ.*, **8**, 69–74.
- Shettle, E. P., and R. W. Fenn, 1979: Models for the aerosols of the lower atmosphere and the effects of humidity variations of their optical properties. AFGLTR 790214, Environ. Res. Paper No. 676, 94 pp.
- Tanre, D., J. F. Geleyn and J. Slingo, 1984: First results of the introduction of an advanced aerosol-radiation interaction in the ECMWF low resolution global model. *Aerosol and Their Climate Effects*. H. E. Gerber and A. Deepak, Eds. Deepak, 133–177.
- Toon, O. B., and J. B. Pollack, 1976: A global average model of atmospheric aerosols for radiative transfer calculations. *J. Appl. Meteorol.*, **15**, 246.
- World Climate Programme, 1984: Report of the experts meeting on aerosols and their climate effects WCP-55. A. Deepak and H. E. Gerber, Eds., WMO, 107 pp.
- Whelpdale, D. M., and R. W. Shaw, 1974: Sulphure dioxide removal by turbulent transfer over grass, snow and water surface. *Tellus*, **26**, 196–205.
- Winkler, P., 1975: Chemical analysis of aitken particles ( $0.2 \mu\text{m}$  radius) over the Atlantic Ocean. *Geophys. Res. Lett.*, **2**, 45–48.